Proceedings of the Institution of Civil Engineers
Geotechnical Engineering 158
July 2005 Issue GE3
Pages 135–144

Paper 13818

Received 19/04/2004
Accepted 10/08/2004

Keywords:
sands/footings & foundations

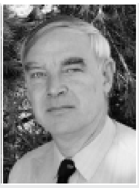

Guy T. Houlsby
Department of Engineering Science, University of Oxford

Byron W. Byrne
Department of Engineering Science, University of Oxford

Design procedures for installation of suction caissons in sand

G. T. Houlsby MA, DSc, FREng, FICE and B. W. Byrne MA, DPhil

Suction-installed caisson foundations are being used or considered for a wide variety of offshore applications ranging from anchors for floating facilities to shallow foundations for offshore wind turbines. In the design of the caissons the installation procedure must be considered as well as the in-place performance. The scope of this paper is to consider the calculations appropriate for the installation of caissons in sands. Calculation methods are presented for determining the resistance to penetration of open-ended cylindrical caisson foundations both with and without the application of suction inside the caisson. Comparisons are made with case records. A companion paper addresses the calculation procedure for installation in clays as well as in other soils.

NOTATION

a	ratio of excess pore pressure at tip of caisson skirt to beneath the base
D	caisson diameter
f	rate of change of diameter over which vertical stress is enhanced
h	installed depth of caisson
h_w	height of water above mudline
K	factor relating vertical stress to horizontal stress
k_f	ratio of permeability within caisson to outside caisson (i.e. $k_f = k_i/k_o$)
L	caisson skirt depth
l	perimeter length of stiffeners within caisson
m	multiple of diameter over which vertical stress is enhanced (i.e. $D_m = mD_o$)
N_q	bearing capacity factor (overburden)
N_γ	bearing capacity factor (self-weight)
p_a	atmospheric pressure
s	suction within caisson with respect to ambient seabed water pressure
t	wall thickness
V, V'	vertical load, effective vertical load
z	vertical coordinate below mudline
δ	interface friction angle
γ, γ'	unit weight of soil, effective unit weight of soil
γ_w	unit weight of water
σ_v, σ'_v	vertical stress, effective vertical stress
ϕ	angle of friction of soil

Subscripts

i	inside caisson
o	outside caisson
s	stiffeners

1. INTRODUCTION

Suction caissons are large cylindrical structures, usually made of steel, open at the base and closed at the top. After an initial penetration into the seabed caused by self-weight, a suction (relative to seabed water pressure) is applied within the caisson, which forces the remainder of the caisson to embed itself, leaving the top flush with the seabed. The purpose of this paper is to present design calculations for the installation of caissons in sand. When the suction is applied, the pressure differential on the lid of the caisson effectively increases the downward force on the foundation. However, in sand the applied suction also generates flow within the soil. The pore pressure gradients are beneficial to the installation process and must be accounted for in the design calculation. Separate calculations are of course necessary to assess the capacity of the caisson once installed—whether used as a shallow foundation or as an anchor. Some of the issues that need to be addressed for the in-service performance of suction caissons in sand are discussed by Byrne and Houlsby.[1–3]

The first major structure installed in dense sand using suction caissons was Statoil's Draupner E riser platform (formerly Europipe 16/11 E) in the North Sea. This was installed successfully during 1994 in 70 m water depth. The caisson foundations were 12 m in diameter and the skirts were 6 m long, and designed to be installed with suction. The design for the installation was based on a combination of field testing, laboratory testing and finite element modelling.[4–6] Statoil installed a second caisson-founded structure in the North Sea in 1996 (Sleipner T). During the detailed design of this structure Erbrich and Tjelta[7] developed a design methodology using design charts based on finite element calculations. The analyses presented in this paper differ from the finite element approach in that they are 'classical' in the sense that they employ simplifying assumptions, borrowing techniques from both pile design and bearing capacity theory. The authors are not aware of any other simplified analysis for installation in sand that has been published. More rigorous analyses, using for instance finite element techniques (as for instance outlined by

Erbrich and Tjelta[7]), could be used for particular installations. The analyses presented here should, however, provide a reasonable approximation for design purposes.

In this paper we address installation in sand, which we treat as drained in the sense that we assume a fully developed steady-state seepage pattern is instantaneously set up for any particular set of hydraulic boundary conditions. This will be a reasonable approximation for reasonably free-draining sands. A companion paper[8] deals with the opposite extreme: where the soil can be treated as fully undrained. The intermediate case of partial drainage is of course much more complex, and we have not attempted this.

2. ANALYSIS

We shall consider a circular caisson of outside diameter D_o and wall thickness t, so that the inside diameter is $D_i = D_o - 2t$. It is useful also to define the mean diameter $D = (D_o + D_i)/2$. For most cases $t << D$, so that $D_o \approx D \approx D_i$. The water depth is h_w, and the vertical coordinate, measured as a depth below mudline, is z. The current embedment of the caisson is h and the height of the caisson is h_c (see Fig. 1). The unit weight of water is γ_w and of the soil is γ. The buoyant unit weight of the soil is $\gamma' = \gamma - \gamma_w$. Atmospheric pressure is p_a.

It is assumed that the net downward vertical load on the caisson, when it is submerged in water, is V'. This is the weight of the caisson, less any buoyant effects and any part of the weight supported by craneage, plus any applied downward loading, for example from the weight of an attached structure. Note that V' will vary with the penetration of the caisson in some way that is unrelated to the following calculations, as more of the attached structure becomes submerged, and as the load taken by a crane is reduced.

The caisson is assumed to be a simple cylinder, although in practice a number of complicating features are often employed, such as:

(*a*) vertical stiffeners attached to the inside of the caisson
(*b*) annular stiffeners attached to the inside of the caisson
(*c*) more complex designs such as stepped caissons.

3. INSTALLATION CALCULATIONS FOR SAND

The installation process can be broken into two components: (a) self-weight penetration, and (b) suction installation. The self-weight penetration in the absence of suction is important, as a seal is necessary at the edge of the foundation in order for the suction component to be performed adequately. The designer will need to understand the interaction between the soil density (and therefore peak friction angle), the skirt wall thickness, and the effective vertical load (V') acting on the foundation so that a sufficient penetration into the sand can be obtained. Once a seal can be ensured, the suction phase can be completed. The designer will need to predict the required suction as a function of depth of penetration. This information can be used to assess pump capacity, and the rate at which suction needs to be applied. The installation contractor will need to appreciate the implications of variations in applied suction, so that effective control of installation is achieved. If the suction is applied too quickly, then localised piping may occur. This could prevent full installation of the foundation. Finally the designer needs to be aware of any limitations to the design, such as the maximum aspect ratio that can be installed with suction while avoiding the possibility of liquefaction of the internal plug of soil. For the purposes of calculation an idealised case of a foundation on a homogeneous deposit of sand (assumed drained) will be considered in this paper.

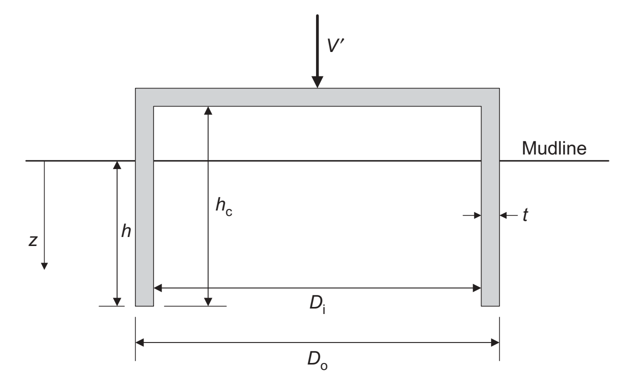

Fig. 1. Outline of suction caisson

3.1. Self-weight penetration

The resistance on the caisson is calculated as the sum of friction on the outside and the inside of the skirt, and the end bearing on the annulus. The frictional terms are calculated in a similar way as in pile design, by calculating the vertical effective stress adjacent to the caisson, and then assuming that horizontal effective stress is a factor K times the vertical effective stress. Assuming that the mobilised angle of friction between the caisson wall and the soil is δ, then we obtain the result that the shear stress acting on the caisson is $\sigma'_v K \tan\delta$. Note that in the subsequent analysis the values of K and δ never appear separately, but only in the combination $K \tan\delta$, so it is not possible to separate out the effects of these two variables. Allowance is made, however, for the possibility of different values of $K \tan\delta$ acting on the outside and inside of the caisson. The difference in the following analysis from conventional pile design is that the contribution of friction in enhancing the vertical stress further down the caisson is taken into account. The end bearing is taken as the sum of N_q and N_γ terms in the conventional way, and it is assumed that solutions for a strip footing of width t are appropriate for the caisson rim.

If (following conventional pile design practice) no account is taken of the enhancement of vertical stress close to the pile due to the frictional forces further up the caisson, then the result for the vertical load on the caisson for penetration to depth h, in the absence of suction, is given by

$$V' = \underbrace{\frac{\gamma' h^2}{2}(K\tan\delta)_o(\pi D_o)}_{\text{friction on outside}} + \underbrace{\frac{\gamma' h^2}{2}(K\tan\delta)_i(\pi D_i)}_{\text{friction on inside}} + \underbrace{\left(\gamma' h N_q + \gamma' \frac{t}{2} N_\gamma\right)(\pi D t)}_{\text{end bearing on annulus}} \tag{1}$$

However, ignoring the enhancement of the stress in this case proves unconservative (i.e. it would underestimate the force and suction required for full penetration), so we develop here a theory that takes this effect into account.

Consider first the soil within the caisson. If we assume that the vertical effective stress is constant across the section of the caisson, then the vertical equilibrium equation for a disc of soil within the caisson (see Fig. 2) leads to the equation

$$\frac{\mathrm{d}\sigma'_{\mathrm{v}}}{\mathrm{d}z} = \gamma' + \frac{\sigma'_{\mathrm{v}}(K\tan\delta)_{\mathrm{i}}(\pi D_{\mathrm{i}})}{\pi D_{\mathrm{i}}^2/4} = \gamma' + \frac{4\sigma'_{\mathrm{v}}(K\tan\delta)_{\mathrm{i}}}{D_{\mathrm{i}}} \tag{2}$$

Writing

$$\frac{D_{\mathrm{i}}}{4(K\tan\delta)_{\mathrm{i}}} = Z_{\mathrm{i}} \tag{3}$$

this equation becomes

$$\frac{\mathrm{d}\sigma'_{\mathrm{v}}}{\mathrm{d}z} - \frac{\sigma'_{\mathrm{v}}}{Z_{\mathrm{i}}} = \gamma' \tag{4}$$

which has the solution

$$\sigma'_{\mathrm{v}} = \gamma' Z_{\mathrm{i}}\left[\exp\left(\frac{z}{Z_{\mathrm{i}}}\right) - 1\right] \tag{5}$$

for $\sigma'_{\mathrm{v}} = 0$ at $z = 0$. The total frictional terms in fact depend on the integral of the vertical effective stress with depth, and we can also obtain

$$\int_0^h \sigma'_{\mathrm{v}}\mathrm{d}z = \gamma' Z_{\mathrm{i}}^2\left[\exp\left(\frac{h}{Z_{\mathrm{i}}}\right) - 1 - \left(\frac{h}{Z_{\mathrm{i}}}\right)\right] \tag{6}$$

For small h/Z_{i} the integral simplifies to $\gamma' h^2/2$.

A similar analysis follows for the stress on the outside of the caisson. We make the simplifying assumptions that: (a) there is a zone between diameters D_{o} and $D_m = mD_{\mathrm{o}}$ in which the vertical stress is enhanced through the action of the downward friction from the caisson; (b) within this zone the enhanced vertical stress does not vary with radial coordinate; and (c) there is no shear stress on vertical planes at diameter D_m. We then obtain the same results as for the inside of the caisson, but with Z_{i} replaced by

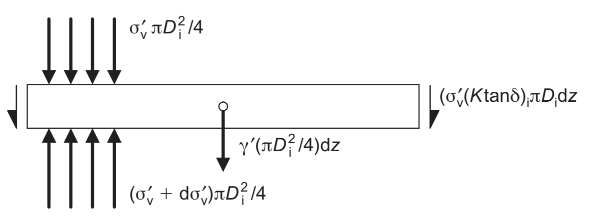

Fig. 2. Equilibrium of slice of soil within caisson

$$Z_{\mathrm{o}} = \frac{D_{\mathrm{o}}(m^2 - 1)}{4(K\tan\delta)_{\mathrm{o}}}. \tag{7}$$

If the more realistic assumption $D_m = D_{\mathrm{o}} + 2f_{\mathrm{o}}z$ is made, where f_{o} is a constant, then

$$Z_{\mathrm{o}} = \frac{D_{\mathrm{o}}\{[1 + (2f_{\mathrm{o}}z/D_{\mathrm{o}})]^2 - 1\}}{4(K\tan\delta)_{\mathrm{o}}} \tag{8}$$

and an analytical solution to the equation

$$\frac{\mathrm{d}\sigma'_{\mathrm{v}}}{\mathrm{d}z} - \frac{\sigma'_{\mathrm{v}}}{Z_{\mathrm{o}}} = \gamma' \tag{9}$$

is not known. The equation can, however, readily be integrated numerically to give the variation of vertical stress with depth. If this approach is adopted then it would be consistent to assume that within the caisson at small z/D the stress is enhanced only in an annulus between D_{n} and D_{i}, where $D_{\mathrm{n}} = D_{\mathrm{i}} - 2f_{\mathrm{i}}z$. This leads to

$$Z_{\mathrm{i}} = \frac{D_{\mathrm{i}}\{1 - [1 - (2f_{\mathrm{i}}z/D_{\mathrm{i}})]^2\}}{4(K\tan\delta)_{\mathrm{i}}} \tag{10}$$

and the differential equation for the vertical stress must again be solved numerically. The resulting solution applies down to a value $z = D_{\mathrm{i}}/2f_{\mathrm{i}}$, at which $D_{\mathrm{n}} = 0$. Below this the original expression for Z_{i} is appropriate.

In equation (1) the end bearing term accounts for a triangular assumed stress distribution across the tip of the caisson (see Fig. 3(a)). Now that the stress inside and outside the caisson may be different, the assumed stress distribution across the tip of the caisson is as in Fig. 3(b). The mean stress on the tip is calculated as follows. First determine σ'_{vo} and σ'_{vi}. For all likely combinations of parameters $\sigma'_{\mathrm{vo}} < \sigma'_{\mathrm{vi}}$; because there is greater enhancement of the stress within the caisson rather than outside. If $\sigma'_{\mathrm{vi}} - \sigma'_{\mathrm{vo}} < 2tN_\gamma/N_{\mathrm{q}}$ then the stress distribution is as shown in Fig. 3(b) and

$$\sigma'_{\mathrm{end}} = \sigma'_{\mathrm{vo}}N_{\mathrm{q}} + \gamma'\left(t - \frac{2x^2}{t}\right)N_\gamma \tag{11}$$

where

$$x = \frac{t}{2} + \frac{(\sigma'_{\mathrm{vo}} - \sigma'_{\mathrm{vi}})N_{\mathrm{q}}}{4\gamma' N_\gamma} \tag{12}$$

If $\sigma'_{\mathrm{vi}} - \sigma'_{\mathrm{vo}} \geqslant 2tN_\gamma/N_{\mathrm{q}}$ then all the flow occurs outwards, $x = 0$ and $\sigma'_{\mathrm{end}} = \sigma'_{\mathrm{vo}}N_{\mathrm{q}} + \gamma' tN_\gamma$.

Accounting for these effects of stress enhancement, equation (1) becomes modified to

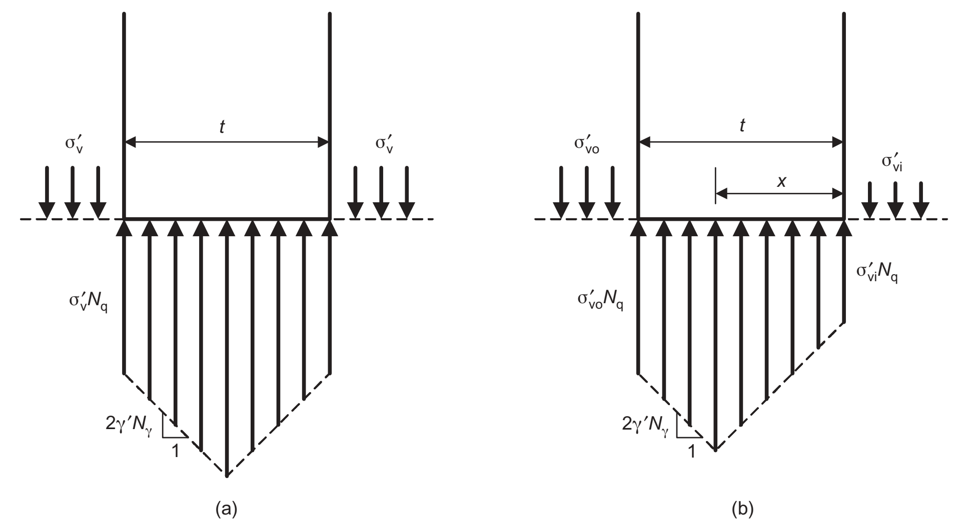

Fig. 3. Stress distribution on caisson tip for (a) equal vertical stresses inside and outside caisson and (b) reduced vertical stress inside caisson

$$V' = \int_0^h \sigma'_{\text{vo}} \mathrm{d}z (K \tan\delta)_{\text{o}} (\pi D_{\text{o}}) + \int_0^h \sigma'_{\text{vi}} \mathrm{d}z (K \tan\delta)_{\text{i}} (\pi D_{\text{i}}) + \sigma'_{\text{end}} (\pi D t) \tag{13}$$

In the special case where m is taken as a constant and uniform stress is assumed within the caisson this can be expressed as

$$V' = \gamma' Z_{\text{o}}^2 \left[\exp\left(\frac{h}{Z_{\text{o}}}\right) - 1 - \left(\frac{h}{Z_{\text{o}}}\right) \right] (K \tan\delta)_{\text{o}} (\pi D_{\text{o}}) + \gamma' Z_{\text{i}}^2 \left[\exp\left(\frac{h}{Z_{\text{i}}}\right) - 1 - \left(\frac{h}{Z_{\text{i}}}\right) \right] (K \tan\delta)_{\text{i}} (\pi D_{\text{i}}) + \sigma'_{\text{end}} (\pi D t) \tag{14}$$

3.2. Suction-assisted penetration

If the pressure in the caisson is s with respect to the ambient seabed water pressure, i.e. the absolute pressure in the caisson is $p_{\text{a}} + \gamma_{\text{w}} h_{\text{w}} - s$, then it is assumed that the excess pore pressure at the tip of the caisson is as: that is, the absolute pressure is $p_{\text{a}} + \gamma_{\text{w}}(h_{\text{w}} + h) - as$. There is therefore an average downward hydraulic gradient of $as/\gamma_{\text{w}} h$ on the outside of the caisson and an upward hydraulic gradient of $(1 - a)s/\gamma_{\text{w}} h$ on the inside. Because the flow is more restricted inside the caisson than outside, a is expected to be a factor somewhat less than 0·5. Calculations for a are presented later in this paper.

We assume that the distribution of pore pressure on the inside and outside of the caisson is linear with depth. The solutions for the vertical stresses inside and outside the caisson are exactly as before, except that γ' is replaced by $\gamma' + as/h$ outside the caisson and by $\gamma' - (1 - a)s/h$ inside the caisson. We further assume that the internal vertical effective stress is reduced sufficiently so that the failure mechanism involves movement of soil entirely inwards ($x = t$ in Fig. 3(b)). The capacity, accounting for the pressure differential across the top of the caisson, is again calculated as the sum of the external and internal frictional terms, and the end bearing terms:

$$V' + s\left(\frac{\pi D_{\text{i}}^2}{4}\right) = \int_0^h \sigma'_{\text{vo}} \mathrm{d}z (K \tan\delta)_{\text{o}} (\pi D_{\text{o}}) + \int_0^h \sigma'_{\text{vi}} \mathrm{d}z (K \tan\delta)_{\text{i}} (\pi D_{\text{i}}) + \left(\sigma'_{\text{vi}} N_{\text{q}} + \gamma' t N_\gamma\right)(\pi D t) \tag{15}$$

where in general the external and internal vertical stresses are determined by numerical integration using the modified values of the effective unit weight on the outside and inside of the caisson.

In the special case where m is taken as a constant and uniform stress is assumed within the caisson this can be expressed as

$$V' + s\left(\frac{\pi D_{\text{i}}^2}{4}\right) = \left(\gamma' + \frac{as}{h}\right) Z_{\text{o}}^2 \left[\exp\left(\frac{h}{Z_{\text{o}}}\right) - 1 - \left(\frac{h}{Z_{\text{o}}}\right) \right] \times (K \tan\delta)_{\text{o}} (\pi D_{\text{o}}) + \left(\gamma' - \frac{(1-a)s}{h}\right) Z_{\text{i}}^2 \left[\exp\left(\frac{h}{Z_{\text{i}}}\right) - 1 - \left(\frac{h}{Z_{\text{i}}}\right) \right] \times (K \tan\delta)_{\text{i}} (\pi D_{\text{i}}) + \left\{ \left[\gamma' - \frac{(1-a)s}{h}\right] Z_{\text{i}} \left[\exp\left(\frac{h}{Z_{\text{i}}}\right) - 1 \right] N_{\text{q}} + \gamma' t N_\gamma \right\} \times (\pi D t) \tag{16}$$

Equations (15) and (16) are each a linear equation in s, and can be used to solve for the suction required to achieve a penetration h.

Note that because of the assumption of pure inward failure, equation (16) does not reduce exactly to equation (13) in the absence of suction. The difference, which is very small, can be resolved as follows. Noting that

$$\sigma'_{vo} = \left(\gamma' + \frac{as}{h}\right) Z_o \left[\exp\left(\frac{h}{Z_o}\right) - 1\right] \quad (17)$$

and

$$\sigma'_{vi} = \left[\gamma' - \frac{(1-a)s}{h}\right] Z_i \left[\exp\left(\frac{h}{Z_i}\right) - 1\right] \quad (18)$$

for $\sigma'_{vo} - \sigma'_{vi} \geqslant 2tN_\gamma/N_q$ then $x = t$ and equation (16) applies. For $\sigma'_{vi} - \sigma'_{v0} \geqslant 2tN_\gamma/N_q$ then $x = 0$ and pure outward flow occurs, and the final term in equation (16) should be replaced by

$$\left\{\left(\gamma' + \frac{as}{h}\right) Z_o \left[\exp\left(\frac{h}{Z_o}\right) - 1\right] N_q + \gamma' t N_\gamma\right\} (\pi D t) \quad (19)$$

For intermediate cases the last term is replaced by $\sigma'_{end}(\pi D t)$, where

$$\sigma'_{end} = \sigma'_{vo} N_q + \gamma' \left(t - \frac{2x^2}{t}\right) N_\gamma \quad (20)$$

and

$$x = \frac{t}{2} + \frac{(\sigma'_{vo} - \sigma'_{vi}) N_q}{4\gamma' N_\gamma} \quad (21)$$

It can be verified that there are smooth transitions between each of these conditions. In each case there is an equation that can be solved for s (for the intermediate case it is a quadratic, in the other cases linear). It can, however, easily be verified that for most cases the outward flow and intermediate solutions apply only for a very small range of penetration at the beginning of the suction process, during which there is a transition in the flow direction of the sand. For practical purposes the transition phase can be ignored.

If the sand is not homogeneous, but consists of a number of layers with different design values of γ', ϕ' and $K \tan \delta$, then the above calculation can be adapted in a reasonably straightforward way, although the integrals for the vertical stress solution become even more cumbersome. Of more significance could be changes of permeability with depth, since this might affect the pore pressure factor a. Caution should therefore be exercised in this case.

3.3. Limits to suction-assisted penetration

As the suction is increased, the upward hydraulic gradient on the inside of the caisson approaches the value at which a piping failure might be induced. At this stage the vertical effective stress inside the caisson at the caisson tip (and in fact throughout the depth of the caisson) falls to zero. It is anticipated that, if attempts were made to increase the suction further, local piping failures would be induced, possibly with a major inflow of water into the caisson, but without significant further penetration. This condition will occur when $\gamma' h - (1 - a)s = 0$, i.e. $s = \gamma' h/(1 - a)$. Substituting this into the penetration equation (equation (16)) (for the simplified vertical stress distribution) and simplifying we obtain

$$V' + \frac{\gamma' h}{(1-a)} \frac{\pi D_i^2}{4} = \frac{\gamma'}{(1-a)} Z_o^2 \left[\exp\left(\frac{h}{Z_o}\right) - 1 - \left(\frac{h}{Z_o}\right)\right] \times (K \tan \delta)_o (\pi D_o) + (\gamma' t N_\gamma)(\pi D t) \quad (22)$$

Solving the above equation for h leads to the maximum depth of penetration that can be achieved using suction. Note because the equation is transcendental in h, and the factor a is a function of h/D, the equation needs to be solved iteratively.

We can observe, however, that the last term is typically small. For small applied vertical loads V', and taking $D_i \approx D \approx D_o$, the above leads to the simple solution

$$h = \frac{4(K \tan \delta)_o Z_o^2}{D} \left[\exp\left(\frac{h}{Z_o}\right) - 1 - \left(\frac{h}{Z_o}\right)\right] \quad (23)$$

If we ignore the effect of stress enhancement, i.e. for small h/Z_o, then

$$\exp\left(\frac{h}{Z_o}\right) - 1 - \left(\frac{h}{Z_o}\right) \approx \frac{h^2}{2Z_o^2} \quad (24)$$

and we obtain

$$h \approx \frac{D}{2(K \tan \delta)_o} \quad (25)$$

This can be used to provide an initial estimate of the maximum achievable penetration with suction. Since $K \tan \delta$ is often approximately 0·5, we conclude that in sand the limit on suction-assisted penetration is likely to be of similar magnitude to the diameter. Note that this limit is much smaller than for installation in clays.[8]

In fact a slightly more stringent limit on suction-assisted penetration can be established on the same basis as the 'reverse bearing capacity' solution used for clays.[8] Again a plastic failure could occur with flow of soil into the caisson and without further penetration. This condition will occur when $\sigma'_{vo} = N_q \sigma'_{vi}$. That is (for the simplified vertical stress distribution):

$$\left(\gamma' + \frac{as}{h}\right) Z_i \left[\exp\left(\frac{h}{Z_i}\right) - 1\right] = N_q \left[\gamma' - \frac{(1-a)s}{h}\right] \times Z_i \left[\exp\left(\frac{h}{Z_i}\right) - 1\right] \quad (26)$$

Although equation (26) provides a more conservative estimate of the limit of suction-assisted penetration, since N_q is usually a large number (typically more than 30), in fact it differs very little from the condition $\gamma' h - (1-a)s = 0$ discussed above.

3.4. The effect of internal stiffeners

The resistance of internal axial stiffening plates can be taken into account by adding resistance terms accounting for the friction and the end bearing on each plate. For the simplified vertical stress distribution the frictional terms will be of the form

$$\gamma' Z_i^2 \left[\exp\left(\frac{h}{Z_i}\right) - 1 - \left(\frac{h}{Z_i}\right) \right] (K \tan \delta)_s l \tag{27}$$

where l is the perimeter length of the stiffeners, and the end bearing terms will be of the form

$$\left\{ \gamma' Z_i \left[\exp\left(\frac{h}{Z_i}\right) - 1 \right] N_q + \gamma' \frac{t_S}{2} N_\gamma \right\} A \tag{28}$$

where t_S is the stiffener thickness and A is the end area of the stiffener. Once suction is applied the friction term is modified by replacing γ' by

$$\gamma' - \frac{(1-a)s}{h} \tag{29}$$

and the end bearing expression becomes

$$\left\{ \left(\gamma' - \frac{(1-a)s}{h} \right) Z_i \left[\exp\left(\frac{h}{Z_i}\right) - 1 \right] N_q + \gamma' \frac{t_S}{2} N_\gamma \right\} A \tag{30}$$

Note the factor $t_S/2$ in this expression rather than t for the caisson wall: this is because the soil flows to either side of the stiffener. Furthermore the influence of the stiffeners alters the expression for Z_i to

$$Z_i = \frac{\pi D_i^2}{4\left[\pi D_i (K \tan \delta)_i + l (K \tan \delta)_s\right]} \tag{31}$$

If the stiffeners do not extend to the base of the caisson then again corrections need to be made to the above expressions to account for this. It should be noted though that the calculations for the vertical effective stress at any level in the caisson then may involve rather cumbersome integrations.

External stiffeners in sand would almost certainly cause problems during installation, as their tips would not be in the region where the effective stress is reduced. As a result they would attract a very large tip resistance. Annular stiffeners, which are often used for caissons in clay, would almost certainly prevent installation in sand.

3.5. Pressure factor *a* and flow calculations

The factor a should be 0·5 for very shallow penetration in a soil of uniform permeability, and would be a function of h/D. As suction is applied there is the possibility that the sand within the caisson might become loosened and thus exhibit a higher permeability. For simplicity one can consider a permeability k_o for the soil outside the caisson and $k_i > k_o$ inside the caisson. The ratio $k_f = k_i/k_o$ will affect the value of a.

Finite element analyses have been used to calculate the value of a in a soil of uniform permeability for a thin-walled caisson for values of h/D up to 0·8 and for values of k_f of 1, 2 and 5. The results of two separate studies (using slightly different mesh details; ref. 9 and Junaideen, 2004, private communication) are shown in Fig. 4.

An approximate fit for $k_f = 1$ is given by

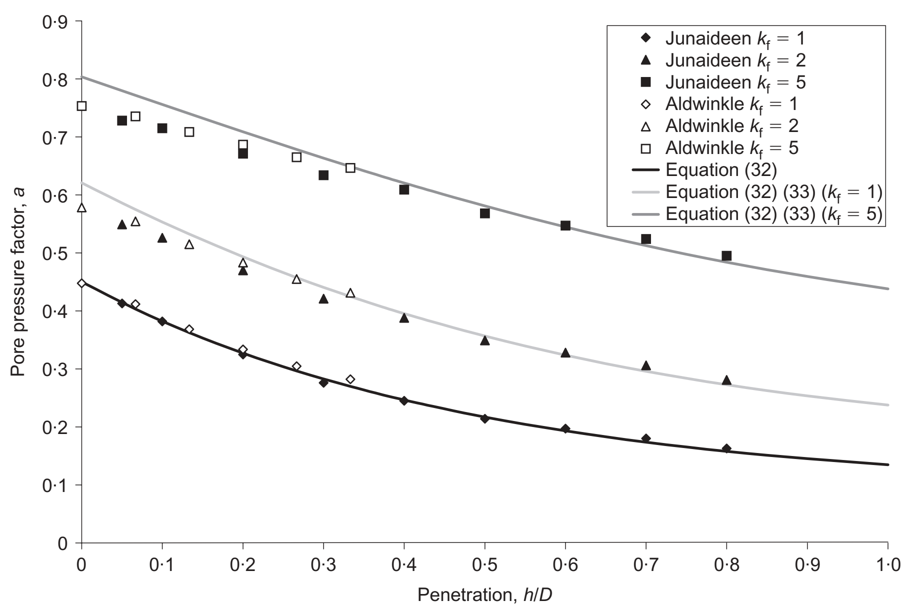

Fig. 4. Variation of pore pressure parameter *a* with *h*/*D* and k_f

32
$$a = a_1 = c_0 - c_1\left[1 - \exp\left(-\frac{h}{c_2 D}\right)\right]$$

with the values $c_0 = 0{\cdot}45$, $c_1 = 0{\cdot}36$, $c_2 = 0{\cdot}48$. This equation captures the trend of the calculations reasonably well, although for $h/D = 0$ the value should theoretically be 0·5 and for very large h/D the factor would be expected to tend to zero.

The effects of different k_f values can be accounted for by a simple calculation in which the head loss within the caisson is reduced in inverse proportion to the permeability. This results in

33
$$a = \frac{a_1 k_f}{(1 - a_1) + a_1}$$

where a_1 is the value from equation (32). Fig. 4 shows a comparison between calculated factors using equations (32) and (33) and numerically calculated factors using finite element analysis.

The flow beneath the caisson due to the suction can be determined using Darcy's law as

34
$$q = \frac{k_o D s}{\gamma_w} F$$

where F is a dimensionless factor that depends on the ratios h/D and k_f. Calculated values of F using finite element analysis (Junaideen, 2004, private communication) are given in Fig. 5. If it is assumed that the excess pressure across the base of the caisson is uniform and of value $-s(1 - a)$, then F can be estimated from the expression $F = (1 - a)\pi k_f/(4h/D)$. The faint lines in Fig. 5 show the computed F values from this expression with a determined by equations (32) and (33), and at large h/D the results from the finite element analysis approach this value. This is because the assumption of uniform pressure across the base of the caisson is reasonable in this case, whereas at shallow depths there is a higher pressure towards the centre of the caisson, resulting in much higher flows in the simplified calculation.

As an example of the flow calculation, for a caisson of diameter 6 m penetrated 4 m into a soil with a uniform permeability of 2×10^{-4} m/s, and with an applied suction of 58 kPa, the estimated flow would be

35
$$\frac{2 \times 10^{-4} \times 6 \times 58}{10} \times 0{\cdot}85 = 0{\cdot}006\text{m}^3/\text{s}$$

If the caisson was installed to this depth in a period of 2 h, then the pumping rate simply to remove the water from the caisson would be

36
$$\frac{\pi \times 3^2 \times 4}{2 \times 3600} = 0{\cdot}016\text{m}^3/\text{s}$$

Such a calculation can be used to assess the relative contributions of the two flow terms to the net required pumping capacity.

The calculations described in the preceding sections have been implemented in a spreadsheet-based program* that has been used for the calculations in the examples below. The information necessary to code the design method is, however, fully specified in this paper, with no additional assumptions

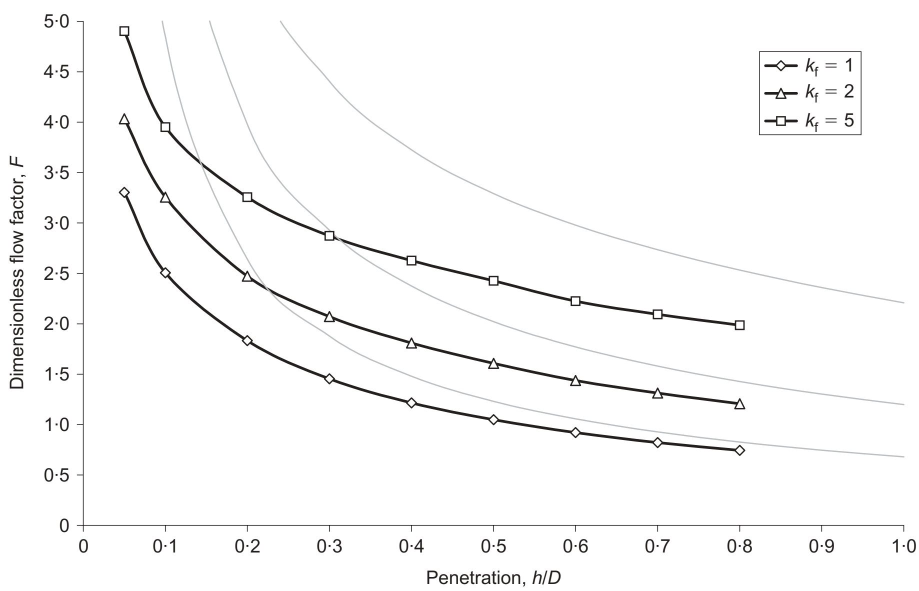

Fig. 5. Variation of dimensionless flow parameter F

* The spreadsheet program SCIP (*S*uction *C*aisson *I*nstallation *P*rediction), which is available from the authors, has been used for all the calculations presented in this paper.

being necessary. The only area where special care is required is the accurate numerical integration of the vertical stress profile. In all these examples the diameter over which the vertical stress is enhanced varies linearly with depth (i.e. the 'loadspread' factors are $f_o = f_i = 1$).

3.6. Example 1: Trial installations at Tenby and Sandy Haven

Results are reported here of two trial installations of caissons made by Offshore Data Ltd at Tenby and Sandy Haven, on the south coast of Wales. At Tenby (Example 1a) a 2m diameter, 2 m high caisson was installed in dense sand. Fig. 6 shows a comparison between the calculated suction and the measured data. The data used for the computations in this and subsequent examples are given in Table 1. It can be seen that the observed suction against penetration response is fitted well, and that the limit to suction-assisted penetration of 1·4 m is also fitted; at this depth no further penetration was observed in spite of an increase in suction.

The second case (Example 1b) is a 4 m diameter caisson, 2·5 m high and with a wall thickness of 20 mm, which was installed at Sandy Haven. Fig. 7 presents the output from the spreadsheet program and compares it with the measured suction against penetration of the caisson. The suction increased approximately linearly with depth up to the full penetration of 2·5 m.

The results from the spreadsheet calculation have been obtained by choosing parameters to fit the data best. The suction against depth curve (which is in fact almost a straight line) depends principally on the values of $K \tan \delta$ and k_f, and very little on other quantities.

Clearly the above figures match very closely the observations at these sites, and all the figures in Table 1 are entirely plausible. Note that for the purposes of the installation a conservative calculation (somewhat unusually) will require *higher* estimates of the strength parameters than might be used for a capacity calculation.

3.7. Example 2: Draupner E

As described in the introduction, this structure was installed by Statoil in 1994 and was the first jacket structure to be installed using suction caissons for the foundation. The soil conditions consist of a very dense sand, and a friction angle of 44° is estimated. As described by Tjelta,[4,6] the foundations consist of 12 m diameter caissons of skirt length 6 m. The wall thickness is taken to be 45 mm. Tjelta[6] describes the installation procedure and states that the self-weight penetration was achieved by flooding the jacket legs, thereby increasing the submerged 'weight' of the structure from 1350 t to 2700 t (i.e. 6622 kN per foundation). Internal stiffeners have been neglected as no information is available about the geometry.

Figure 8 shows the predictions as given by the spreadsheet program compared with the range of field measurements as obtained on site for the four caissons and reported by Tjelta.[6]. The permeability factor $k_f = k_i/k_o$ was taken as 3·0 to provide a good correlation between the case record and the calculated suction pressures. As can be seen in Table 1, values of this factor in the range 2·0 to 3·0 were found appropriate in all cases studied. This indicates that there is probably some loosening of the sand within the caisson due to the upward flow of water, causing an increase in the permeability. Although it is not taken into account in the analysis, it is possible that this loosening occurs principally in a zone close to the caisson wall.

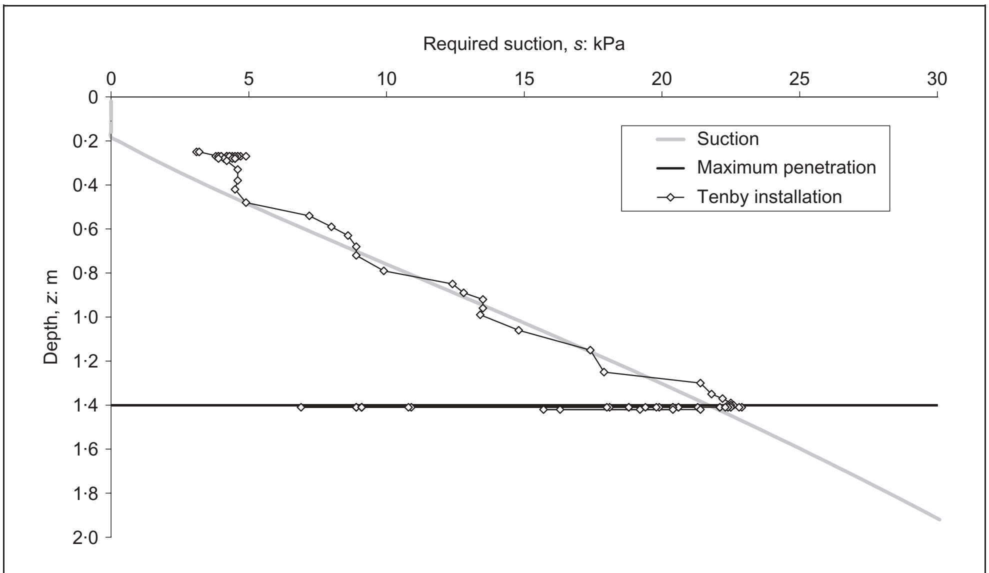

Fig. 6. Calculated suction and case record for Tenby installation, Example 1a

3.8. Example 3: Sleipner T

The Sleipner T structure was the second jacket to be installed by Statoil in the North Sea. The foundations

Example	Location	D: m	L: m	t: mm	V': kN	ϕ': deg	γ': kN/m^3	$K \tan \delta$	k_i/k_o
1a	Tenby	2·0	2·0	8	10	40	8·5	0·48	3·0
1b	Sandy Haven	4·0	2·5	20	100	40	8·5	0·48	2·0
2	Draupner E	12·0	6·0	45	6622	44	8·5	0·63	3·0
3	Sleipner T	15·0	5·0	45	12000	45	8·5	0·8	3·0
4	Laboratory tests	0·15	0·2	1·65	variable	45	8·5	0·45	2·5

Table 1. Data used for spreadsheet calculations

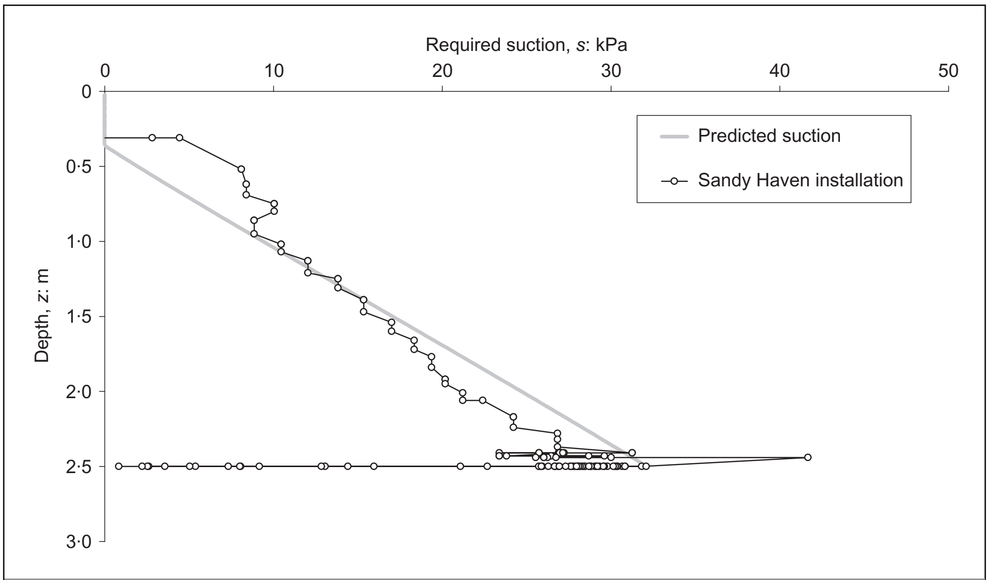

Fig. 7. Calculated suction and case record for Sandy Haven installation, Example 1b

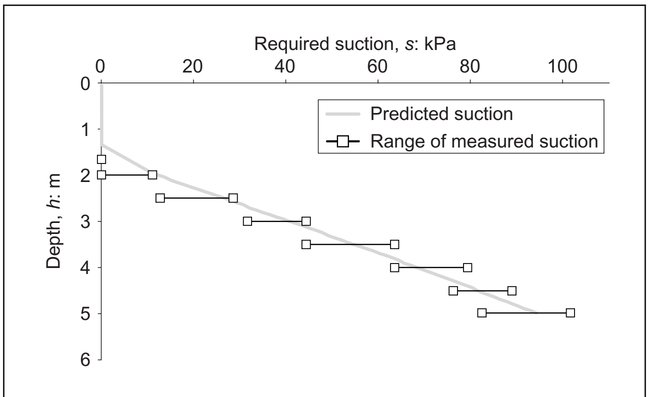

Fig. 8. Calculated and measured suction at Draupner E, Example 2

are 15 m in diameter and the skirt depth is 5 m.[5,10] The wall thickness is taken to be 45 mm and again the internal stiffeners are neglected as there is insufficient information available on this detail. The soil conditions consist of a very dense sand, and a friction angle of 45° is used in the calculations. Lacasse[10] presents measured data from the installation, which show that the self-weight penetration is about 1·95 m. It is possible to use this information to back-calculate the effective vertical load applied to each foundation as this is not given in the literature. An effective vertical load per foundation of 12 MN gives the appropriate self-weight penetration, and this corresponds to a weight of the jacket of about 48 MN, which is reasonable. Using the parameter values in Table 1 provides a good fit to the range of data on observed suction as reported by Lacasse,[10] as shown in Fig. 9.

3.9. Example 4: Laboratory tests

This final example, shown in Fig. 10, reports laboratory-scale tests by Sanham.[11] The caisson foundation is 150 mm in diameter with a skirt length of 200 mm (so that, unlike the previous cases, the L/D ratio is greater than 1). The applied vertical load in three tests reported here was 45 N, 85 N and 165 N giving a self-weight penetration of approximately 28 mm, 49 mm and 79 mm. In this particular case, owing to the combination of the different variables, it is possible for the foundation to be installed, even though the L/D ratio is greater than 1·0. Fig. 10 shows the three suction against penetration curves, compared with the theoretical calculations. The spreadsheet calculation captures the trend of variation between the curves as a function of the applied load.

The examples show that, with plausible choice of input parameters, the presented method of analysis fits case records of installation in sand well. It is appreciated that there are, of course, a number of parameters on which the calculation depends, so that to a large extent this match can be achieved by careful choice of

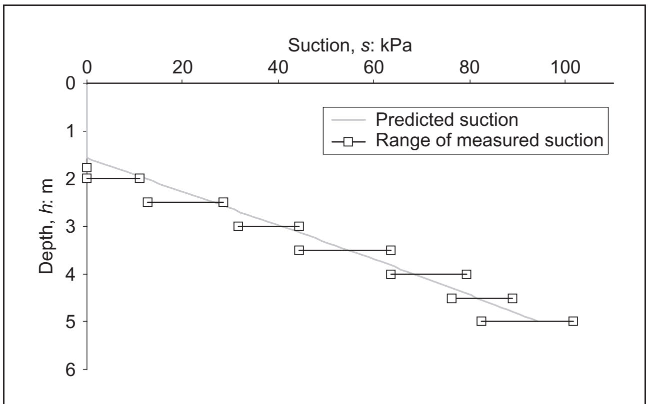

Fig. 9. Calculated and measured suction at Sleipner T, Example 3

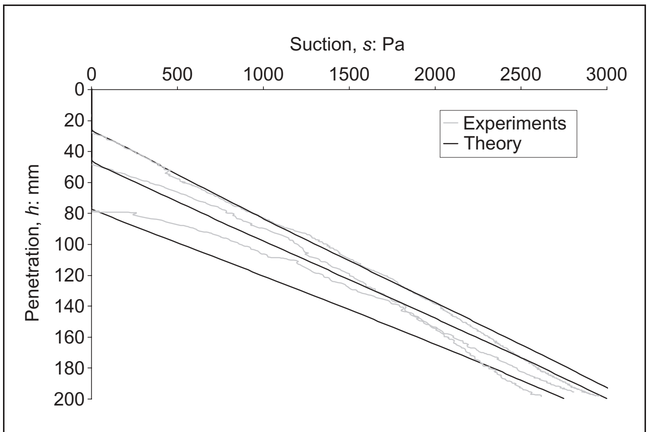

Fig. 10. Calculated and measured suction in laboratory, Example 4

parameters. The solution for the suction depends (as might be expected) significantly on the choice of the value of $K \tan \delta$, and it was found in four of the five examples that a choice of $K \tan \delta = 0{\cdot}54 \pm 0{\cdot}09$ was appropriate, indicating a fairly narrow range of values of this important parameter. One case (Sleipner T) required a much higher value of $K \tan \delta = 0{\cdot}8$. The reason for this is uncertain, but it may be related to the fact that unusually high cone resistances were encountered at shallow depth at this site. The probable explanation is that not only is the sand dense, but the *in situ* $K_o = \sigma'_h / \sigma'_v$ is also though to be high. Both of these factors may have led to the high $K \tan \delta$ value. For the method described here to be a useful predictive tool, clearly further experience must be gained on appropriate parameter selection.

4. CONCLUSIONS

In this paper we present a series of design calculations that can be used to assess the installation of skirted foundations installed into sand using suction. The calculations cover self-weight penetration, suction-assisted penetration, and an assessment of the limitations to the suction installation process. These calculations have been implemented in a spreadsheet program to enable predictions of installation to be made. In the final part of the paper we compare the predictions with four case records, and a good agreement is found with the measured data.

5. ACKNOWLEDGEMENTS

B. W. B. acknowledges generous support from Magdalen College, Oxford. The authors are grateful to Zeena Junaideen, who carried out the finite element calculations reported in Figs 4 and 5, and to Rob Ellis of Offshore Data Ltd for supplying the data used in Examples 1a and 1b.

REFERENCES

1. Byrne B. W. and Houlsby G. T. Experimental investigations of the response of suction caissons to transient vertical loading *Proceedings ASCE, Journal of Geotechnical and Geoenvironmental Engineering*, 2002, **128**, No. 11, 926–939.
2. Byrne B. W. and Houlsby G. T. Foundations for offshore wind turbines. *Philosophical Transactions of the Royal Society of London, Series A*, 2003, **361**, 2909–2930.
3. Byrne B. W. and Houlsby G. T. Experimental investigations of the response of suction caissons to transient combined loading. *Proceedings ASCE, Journal of Geotechnical and Geoenvironmental Engineering*, 2004, **130**, No. 3, 240–253.
4. Tjelta T. I. Geotechnical aspects of bucket foundations replacing piles for the Europipe 16/11-E Jacket. *Offshore Technology Conference*, Houston, TX, 1994, Paper OTC 7379.
5. Bye A., Erbrich C. T., Rognlien B. and Tjelta T. I. Geotechnical design of bucket foundations. *Offshore Technology Conference*, Houston, TX, 1995, Paper OTC 7793.
6. Tjelta T. I. Geotechnical experience from the installation of the Europipe Jacket with bucket foundations. *Offshore Technology Conference*, Houston, TX, 1995, Paper OTC 7795.
7. Erbrich C. T. and Tjelta T. I. Installation of bucket foundations and suction caissons in sand: geotechnical performance. *Offshore Technology Conference*, Houston, TX, 1999, Paper OTC 10990.
8. Houlsby G. T. and Byrne B. W. Design procedures for installation of suction caissons in clay and other materials. *Geotechnical Engineering*, 2005, **158**, No. 2, 75–82.
9. Aldwinkle C. G. *The Installation of Offshore Plated Foundations for Oil Rig.* Department of Engineering Science, Oxford University, 1994, Final Year Project Report.
10. Lacasse S. Ninth OTRC Honors Lecture: Geotechnical contributions to offshore development. *Offshore Technology Conference*, Houston, TX, 1999, Paper OTC 10822.
11. Sanham S. C. *Investigations into the Installation of Suction Assisted Caisson Foundation.* Department of Engineering Science, Oxford University, 2003, Final Year Project Report.

What do you think?
To comment on this paper, please email up to 500 words to the editor at journals@ice.org.uk

Proceedings journals rely entirely on contributions sent in by civil engineers and related professionals, academics and students. Papers should be 2–5000 words long, with adequate illustrations and references. Please visit www.thomastelford.com/journals for author guidelines and further details.